MOLECULAR AND CELLULAR BIOLOGY, Aug. 2003, p. 5475–5488 Vol. 23, No. 16
0270-7306/03/$08.00+0 DOI: 10.1128/MCB.23.16.5475–5488.2003

Epigenetic Properties and Identification of an Imprint Mark in the Nesp-Gnasxl Domain of the Mouse *Gnas* Imprinted Locus

Candice Coombes,[1]† Philippe Arnaud,[1] Emma Gordon,[1] Wendy Dean,[1] Elizabeth A. Coar,[1] Christine M. Williamson,[2] Robert Feil,[3] Jo Peters,[2] and Gavin Kelsey[1]*

Developmental Genetics Programme, The Babraham Institute, Cambridge CB2 4AT,[1] and MRC Mammalian Genetics Unit, Harwell, Didcot, Oxfordshire OX11 0RD,[2] United Kingdom, and Institute of Molecular Genetics, CNRS, UMR-5535, 34293 Montpellier, France[3]

Received 20 December 2002/Returned for modification 7 April 2003/Accepted 20 May 2003

The *Gnas* locus in the mouse is imprinted with a complex arrangement of alternative transcripts defined by promoters with different patterns of monoallelic expression. The Gnas transcript is subject to tissue-specific imprinted expression, Nesp is expressed only from the maternal allele, and Gnasxl is expressed only from the paternal allele. The mechanisms controlling these expression patterns are not known. To identify potential imprinting regulatory regions, particularly for the reciprocally expressed Nesp and Gnasxl promoters, we examined epigenetic properties of the locus in gametes, embryonic stem cells, and fetal and adult tissues. The Nesp and Gnasxl promoter regions are contained in extensive CpG islands with methylation of the paternal allele at Nesp and the maternal allele at Gnasxl. Parental allele-specific DNase I-hypersensitive sites were found at these regions, which correlate with hypomethylation rather than actual expression status. A germ line methylation mark was identified covering the promoters for Gnasxl and the antisense transcript Nespas. Prominent DNase I-hypersensitive sites present on paternal alleles in embryonic stem cells are contained within this mark. This is the second gametic mark identified at *Gnas* and suggests that the Nesp and Gnasxl promoters are under separate control from the Gnas promoter. We propose models to account for the regulation of imprinting at the locus.

Genomic imprinting in mammals results in the unequal expression of the two alleles, strictly according to parental origin, of a small subset of genes (39, 43). At present, some 70 imprinted genes have been identified in the mouse, with a similar number in humans, most genes residing in clusters (31; C. V. Beechey et al., unpublished data [http://www.mgu.har.mrc.ac.uk/imprinting/imprinting.html]). Inappropriate expression of many of these genes (lack of expression, or loss of imprinting) results in various anomalous phenotypes, many of which affect fetal growth and placental function (39, 51).

One of the first imprinted effects described was identified from uniparental inheritance of the distal region of chromosome (Chr) 2 in the mouse (7). Maternal and paternal duplications of this region were found to cause striking and superficially opposite neonatal phenotypes, with behavioral and morphological effects. Through the use of a number of reciprocal translocations, the region responsible for the imprinted phenotypes was narrowed down to an ~7-Mb interval (36, 53), and by methylation-sensitive representational difference analysis, we subsequently identified a complex imprinted cluster at the *Gnas* locus (24, 37). *Gnas* encodes the stimulatory G-protein subunit Gsα. In addition to the coding transcript for Gsα, the locus was found to comprise two imprinted transcripts: Nesp expressed from the maternal allele (which codes for the chromogranin-like neuroendocrine secretory protein NESP55 [21]) and Gnasxl expressed from the paternal allele (which codes for XLαS, a variant Gsα that has a large noncanonical amino-terminal domain [23]). These two transcripts arise from alternative upstream promoters, and both transcripts are spliced to exon 2 of *Gnas* and contain downstream exons in common with *Gnas*. Additional complexity of the locus has emerged from identification of a noncoding transcript, Nespas, which runs antisense to Nesp (27, 54, 55), and an alternative noncoding first exon for *Gnas* with paternal-specific expression (29). The human *GNAS* locus has a very similar organization (17–19, 28).

Imprinting of *GNAS* had been implicated from the different clinical manifestations of inactivating mutations of Gsα, which cause the autosomal dominant disorder Albright's hereditary osteodystrophy (8, 52). Maternally inherited mutations in *GNAS* are associated with multihormone resistance, a condition referred to as pseudohypoparathyroidism type 1a (PHP1a), because patients present with renal resistance to parathyroid hormone. Tissue-specific imprinting in both humans and mice has subsequently been described, with exclusive or prominent expression of the maternal allele in sites such as proximal renal tubules, brown and white adipose tissue, and the pituitary and thyroid glands (13, 16, 30, 61). Imprinting in these target tissues accounts for some of the endocrine anomalies (52). The Nesp and Gnasxl promoters, in contrast, display monoallelic expression at all sites in which they are expressed (18, 19, 27, 37).

The *cis*-acting elements that control imprinting at the *Gnas* and *GNAS* clusters and the mechanisms by which monoallelic expression of the various promoters is executed are not known. Imprinted control regions (ICRs) defined by deletion analysis at other loci coincide with differentially methylated regions

* Corresponding author. Mailing address: Developmental Genetics Programme, The Babraham Institute, Cambridge CB2 4AT, United Kingdom. Phone: 44-1223 496332. Fax: 44-1223 496022. E-mail: gavin.kelsey@bbsrc.ac.uk.

† Present address: Johns Hopkins University, Baltimore, MD 21231.

(DMRs), where the methylation state of the two parental alleles differs markedly (11, 48, 56, 60) and where methylation of one allele is laid down in the respective germ line (41, 45, 50, 59). Female germ line methylation at imprinted loci depends upon the DNA methyltransferases Dnmt3a and Dnmt3b and the related protein Dnmt3l (6, 15), but the sequence features that specify DMRs for methylation in either germ line are not known. Direct repeats often found within or adjacent to DMRs have been implicated on the basis that such repeats are not found in CpG islands of nonimprinted genes (32) or nonimprinted homologues in other species (33, 34). Such direct repeats have been noted at the human *GNAS* locus in the NESP55 and XLαS exons (18, 19). Ultimately, differential methylation, in concert with specific chromatin organization at ICRs, is translated into monoallelic expression of linked promoters in somatic tissues by a variety of mechanisms (39, 43).

Three DMRs have been identified at *Gnas* and *GNAS*. The Nesp DMR has paternal methylation, while the Gnasxl DMR and a DMR covering *Gnas* exon 1A (also referred to as exon A/B) have maternal methylation (18, 19, 24, 28, 29, 37). The exon 1A DMR has been shown to be a gametic methylation mark in the mouse (29); the equivalent human region may also be a primary DMR (22). The control of tissue-specific imprinting of the Gsα-coding transcript may reside in the exon 1A region, as patients with hormone resistance in the absence of the other features of Albright's hereditary osteodystrophy (a condition known as PHP1b) almost invariably display altered methylation at exon 1A (3, 28). Whether this DMR controls imprinting of the entire complex locus is not clear: PHP1b patients may or may not also show altered methylation at the NESP55 and XLαS DMRs. Here, we present a characterization of the epigenetic properties of the mouse *Gnas* locus as a means of pinpointing potential ICRs and predicting their possible modes of actions. We have mapped the extent of differential methylation at the Nesp and Nespas/Gnasxl DMRs, examined gross chromatin organization as revealed by DNase I sensitivity, and identified a second germ line DMR.

MATERIALS AND METHODS

Sequence analysis. The sequence of the mouse Nesp-Gnasxl region analyzed was AJ251761 (17), with additional sequence from the mouse BAC clone RP23-439H2 (AL593857). All sequence positions given correspond to AJ251761. CpG islands were mapped using CPGPLOT in the EMBOSS package. Direct repeated sequences were located using Compare (in the GCG10 suite of the Genetics Computer Group available through the BBSRC Bioscience IT Service) and Tandem Repeats Finder (5) and were aligned by visual inspection. Transcription factor binding site motifs were identified using Match available at BIOBASE GmbH (http://www.gene-regulation.com). Additionally, potential binding sites for CTCF were identified using the consensus CCGCNNGGNGNC (57) and CCGCNNGGNGGCAG (A. Ferguson-Smith, personal communication) and for YY1 using GCGCCATCTTGANT (26), in each case allowing up to three mismatches from these consensuses.

Collection of gametes and early embryos. Oocytes were obtained from juvenile F_1 (C57BL/6J × CBA/Ca) mice; morulae and blastocysts were obtained from an $F_1 \times F_1$ cross, except where indicated. Oocytes were collected from superovulated immature females, as described by Hogan et al. (20). Mature spermatozoa were isolated from epididymis of adult CBA/Ca mice.

ES cells. Embryonic stem (ES) cells used in this study have been described previously (9). Hybrid ES cell line SF1-1 was obtained from $F_1 \times$ *Mus spretus* hybrid blastocysts created by in vitro fertilization. Monoparental ES cell lines used were AG-A (androgenetic) and PR-8 (parthenogenetic). Cells were cultured on gelatin-coated flasks (0.1% gelatin) with feeder cells (γ-irradiated primary embryonic fibroblasts) at 37°C under 5% CO_2, in Iscove's modified Dulbecco's modified Eagle medium supplemented with 15% fetal calf serum, recombinant mouse leukemia inhibitory factor (20 ng/ml), penicillin (50 U/ml), streptomycin (50 μg/ml), 0.1 mM β-mercaptoethanol, 1× modified Eagle medium, nonessential amino acids, and 2 mM glutamine. Prior to harvesting, ES cells were passaged onto gelatin-coated flasks in the absence of feeders to reduce their contribution to the final cell pellet.

Southern analysis of methylation. Embryos (12.5 days postcoitum [dpc]) with uniparental partial disomy for distal Chr 2 were generated by standard methods of intercrossing reciprocal translocation heterozygotes and have been described before (24, 37). DNAs (10 μg per reaction) were digested with the enzymes indicated, together with *Bsh*1236I, *Hin*6I, *Hpa*II, or *Msp*I, resolved by electrophoresis on 1% agarose–TAE gels (TAE is 40 mM Tris-acetate, 10 mM EDTA), and transferred by capillary blotting onto charged nylon membranes. Probes were restriction fragments subcloned into pBluescript II KS(+) (Stratagene) from genomic phage and cosmids for Nesp and Gnasxl (24). Hybridizations were performed with gel-purified probes labeled with [α-^{32}P]dCTP (ICN) by random priming.

Bisulfite sequence analysis. Oocytes (200 to 600), morulae (5 to 20), or blastocysts (5 to 8) were resuspended in 32.5 μl of a solution containing 10 μg of glycogen, 1 mM sodium dodecyl sulfate, and proteinase K (280 μg/ml) and were incubated for 90 min at 37°C and then for 15 min at 95°C in a thermocycler. The resulting DNA lysate was denatured by addition of 1.1 μl of 10 N NaOH and incubation at 50°C for 15 min. For bisulfite treatment, 200 μl of ~4 M sodium bisulfite, pH 5.0 (final concentration, ~3.5 M; Sigma); 1.5 μl of 75 mM hydroquinone (final concentration, 0.5 mM; Sigma); and 5 μg of glycogen were added, and DNA incubated at 55°C for 4 h. Desalting was carried out using the QIAquick PCR purification kit (Qiagen), and eluted DNA (in 50 μl Tris-HCl, pH 7.5) was desulfonated by treatment with 1.6 μl of 10 N NaOH. DNA was ethanol precipitated and resuspended in H_2O (5 μl per 100 cell equivalents). A nested primer strategy was used to amplify bisulfite-treated oocyte and early embryo DNA. PCR, cloning, and sequencing were performed as previously described (44). Primer sequences are available on request. Prior to cloning, PCR products were tested for full conversion and methylation status by pilot digestion with appropriate restriction enzymes.

Isolation of nuclei and DNase I sensitivity analysis. Tissues for isolation of nuclei were obtained from (C57BL/6J × *M. spretus*) mice and the backcross offspring from (C57BL/6J × *M. spretus*) females to C57BL/6J males (the latter were genotyped by PCR for the presence of *M. spretus* alleles at *D2Mit22* and *D2Mit74*). Nuclei were isolated from frozen tissues (brain, liver or kidney) after disruption under liquid nitrogen and homogenization, as described elsewhere (25). For ES cells, 5×10^7 to 5×10^8 cells were harvested for preparation of nuclei and treated as previously described (25). DNase I digestion of nuclei was performed immediately after isolation. Nuclei (aliquots of ~10^7 suspended in 200 μl of 60 mM KCl, 15 mM NaCl, 5 mM $MgCl_2$, 0.1 mM EGTA, 15 mM Tris-HCl [pH 7.5], 0.5 mM dithiothreitol, 0.3 M sucrose, 5% [vol/vol] glycerol) were treated with DNase I (Roche grade I) at 0 to 750 U/ml at 25°C for 10 min. Digestion was stopped by addition of a solution containing 200 μl of 20 mM EDTA, 1% (wt/vol) sodium dodecyl sulfate, and proteinase K (200 μg/ml) and treatment at 50°C for 16 h. DNA was purified by extraction with phenol-chloroform-isoamylalcohol (25:24:1) and chloroform-isoamylalcohol (24:1), precipitated with ethanol, and resuspended in 10 mM Tris-HCl–1 mM EDTA (pH 8.0). For detection of DNase I-hypersensitive sites (HSSs), 20 μg of each treated DNA was digested with appropriate restriction enzymes, electrophoresed, blotted and hybridized as above. Probes were PCR fragments labeled directly with [α-^{32}P]dCTP (ICN) by random priming (primer details available on request).

RESULTS

Extent of differential methylation at the mouse Nesp-Gnasxl domain. In this study we focused on the imprinted domain spanning the promoters for the maternally expressed Nesp transcript and for the paternally expressed Gnasxl and Nespas transcripts. We previously identified that the Nesp exons reside within a region of paternal methylation and the Gnasxl exon within a region of maternal methylation (24, 37). Comparable DMRs are present at the corresponding human locus (18, 19). It was not clear, however, how extensive these DMRs were, or whether additional regions of parental allele-specific methylation existed at the locus. As shown schematically in Fig. 1A, the Nesp and Gnasxl promoters are alternative and oppositely imprinted promoters for *Gnas*, as the Nesp and Gnasxl exons

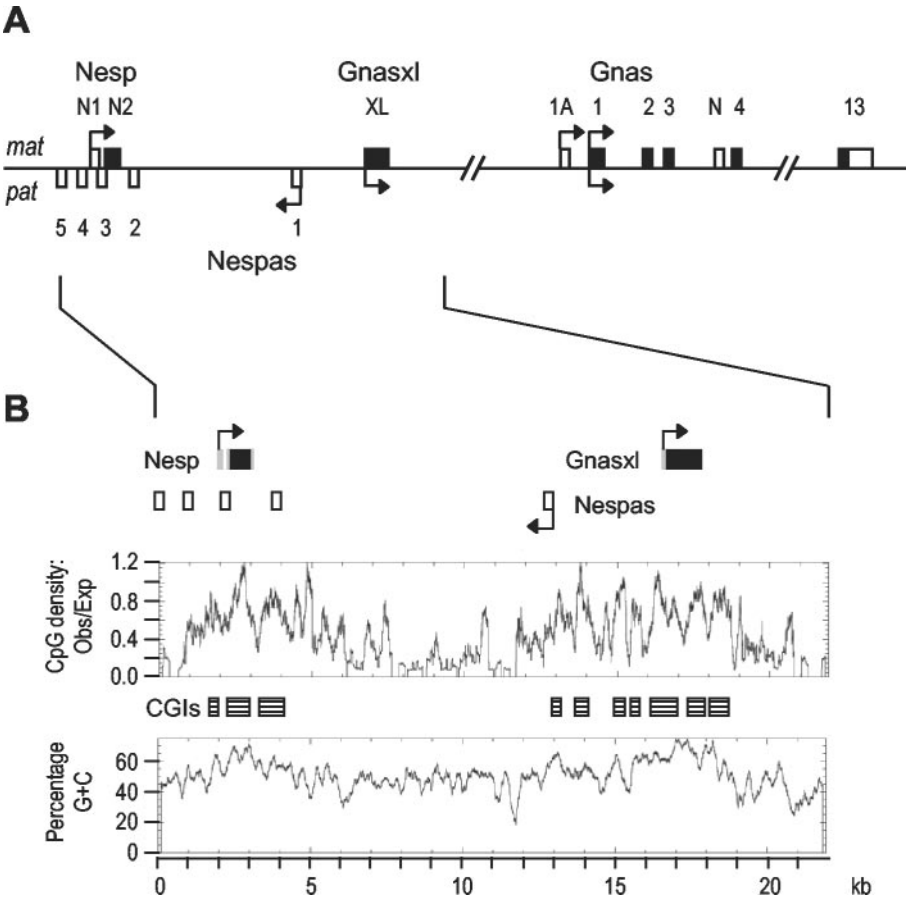

FIG. 1. The Nesp-Gnasxl domain of the *Gnas* imprinted cluster. (A) Schematic overview of the mouse *Gnas* locus. Exons of the Nesp, Gnasxl and Gnas transcripts are shown above the line (for simplicity, not all Gnas exons are shown): coding regions are filled, noncoding regions open. Exons for the Nespas antisense transcript are shown below the line. Promoters are indicated by horizontal arrows, with those maternally expressed (*mat*) shown above the line and those paternally expressed (*pat*) shown below the line. The Nesp and Gnasxl exons are 48.8 and 34.0 kb upstream of Gnas exon 2, respectively, onto which they are both spliced. (B) Sequence properties of the Nesp-Gnasxl domain. A graphical output of sequence AJ251761 analyzed by CPGPLOT is shown. CpG islands (CGIs) are identified as boxes.

are spliced on to exon 2 of *Gnas*. Nespas is an imprinted noncoding transcript which runs antisense to Nesp (27, 54, 55).

The Nesp, Nespas, and Gnasxl promoters are each embedded within CpG island clusters (Fig. 2B): the Nesp CpG island region extends over 2.4 kb; the Nespas and Gnasxl promoters are contained in an extensive CpG island region spanning 5.8 kb. Direct repeats are present in both CpG island regions (Table 1). The repeat in Nesp is based on the 12-mer GAGA CCGAGCCN repeated 10 times, which coincides with a peak of CpG density within the CpG island. It is within the coding exon, and conserved in other species (19), and encodes reiterated glutamic acid, threonine and proline residues in the Nesp polypeptide. The Gnasxl exon contains two regions of CG-rich tandem repeats: six copies of a 36-mer and five copies of an 18-mer (Table 1). Both contribute to alanine rich parts of the XLαS domain. The human XLαS exon contains similar CG-rich repeats (Table 1) (18). The Nesp or Gnasxl repeats do not comprise reiterations of good matches to transcription factor binding site motifs, in particular, multiple sites for the insulator and boundary factors CTCF and YY1 are absent. Two less reiterated tandem repeats (a 16-mer at 19363 to 19399 and a 24-mer at 21631 to 21687), which do not contribute CpG dinucleotides, are located downstream of the Gnasxl exon and CpG islands.

To assay methylation across the Nesp-Gnasxl domain Southern blot analysis was done using DNAs from 12.5-dpc embryos having maternal duplication or paternal duplication for distal Chr 2 [designated MatDp(dist2) and PatDP(dist2), respectively]. The DNAs were cleaved with one or more of the methylation-sensitive restriction enzymes *Hpa*II (CCGG), *Hin*6I (GCGC), and *Bsh*1236I (CGCG), none of which cleave when their recognition sites contain ^{Me}CpG. Representative Southern blots are shown in Fig. 2. The region immediately upstream of Nesp (analyzed with probe N7 on a 15.4-kb *Bam*HI fragment) has a low CpG density and few assayable sites, but is highly methylated on both maternal and paternal alleles. We also checked methylation over most of the 85 kb further upstream and did not detect regions of differential methylation (data not shown). The 5′ boundary of the Nesp DMR is seen with probe N7 on a *Hin*dIII digest (Fig. 2B), while the 3′ boundary was mapped with probe SX2 on an *Eco*32I fragment (data not shown). The paternally methylated DMR thus extends ~4.4 kb, covering the two Nesp exons and the CpG islands. Downstream of the Nesp DMR, CpG density declines

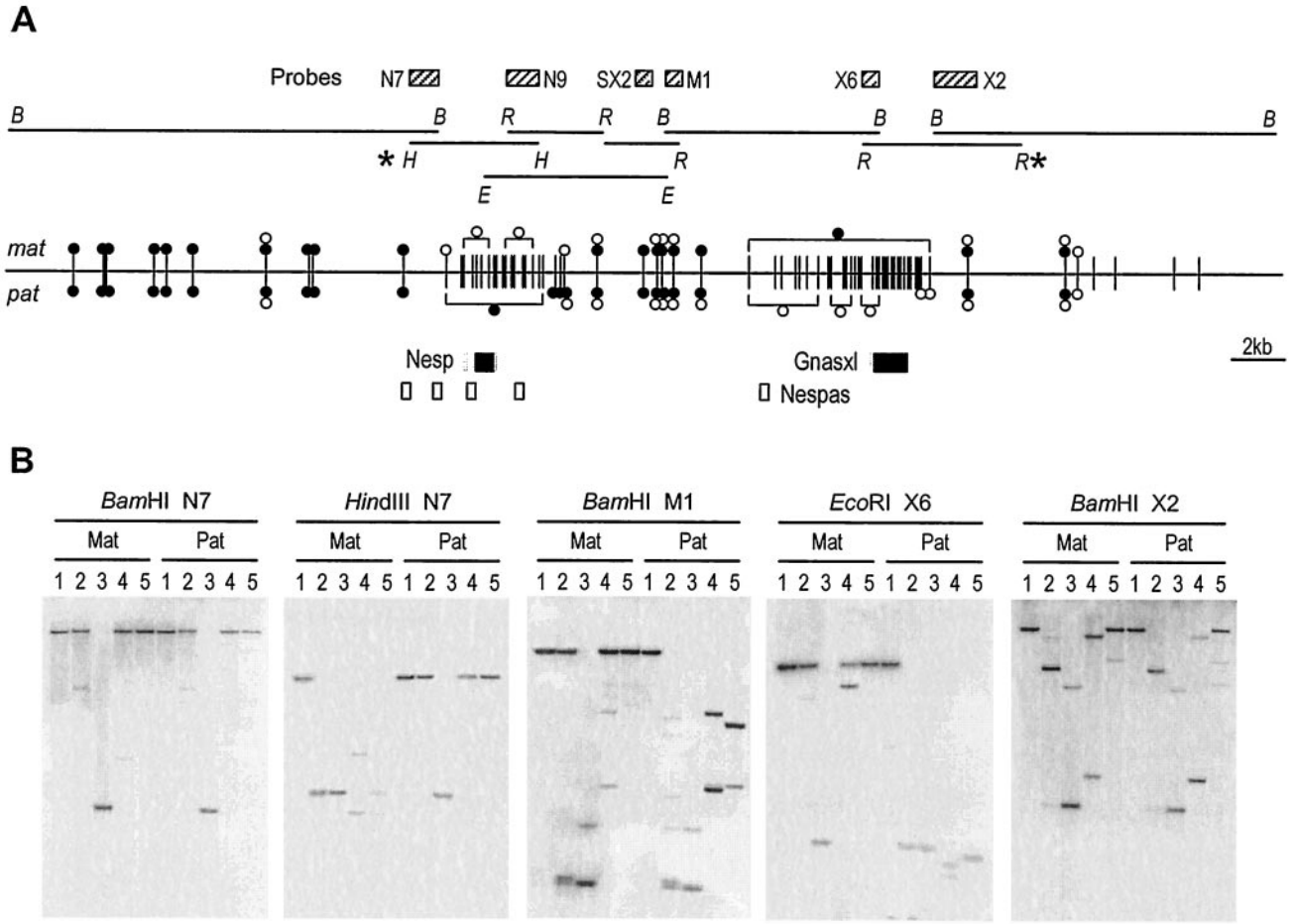

FIG. 2. Extent of differential methylation across the Nesp-Gnasxl domain. (A) The restriction fragments analyzed on Southern blots are indicated by the horizontal lines, and the respective restriction enzyme sites are abbreviated as follows: *B*, *Bam*HI; *E*, *Eco*32I; *H*, *Hin*dIII; and *R*, *Eco*RI. The probes used are shown as striped boxes. Below, the methylation status of *Hpa*II sites in 12.5-dpc embryo DNAs is summarized. Each vertical line represents a single *Hpa*II site (in a few cases, two inseparable sites). Methylation is given separately on the maternal (*mat*) and paternal (*pat*) alleles, where filled circles represent fully methylated, open circles represent unmethylated, and paired circles represent partially methylated. Those sites grouped in square brackets are all methylated or unmethylated, as indicated. For sites without symbols, methylation state could not be determined. Methylation status was also assayed for many *Hin*6I and *Bsh*1236I sites, which did not differ appreciably from that for *Hpa*II, but is not shown for the sake of clarity. The methylation summary includes results from difference product clones (24). The AJ251761 sequence analyzed in Fig. 2B extends between the *Hin*dIII and *Eco*RI sites marked (*); the outer *Bam*HI (*B*) sites are situated at 82392 and 36822 in the sequence of mouse BAC RP23-439H2 (AL593857). (B) Representative Southern blots showing digests of 12.5-dpc MatDp(dist2) (Mat) and PatDp(dist2) (Pat) embryo DNAs hybridized with the probes indicated. DNAs are digested with the restriction enzymes indicated above each blot in combination with no other enzyme (lane 1), *Hpa*II (lane 2), *Msp*I (lane 3), *Hin*6I (lane 4), or *Bsh*1236I (lane 5).

(Fig. 1B) and an ~4.0-kb region contains sites with full or partial methylation on both maternal and paternal alleles. Further downstream, there is a transition region in which the paternal allele shows less complete methylation before the very low level of methylation that characterizes the DMR (probe M1 on a *Bam*HI digest; Fig. 2B). Methylation on the maternal allele is extensive (probe X6 on a *Eco*RI digest [Fig. 2B]), spanning ~6.6 kb, including both Nespas and Gnasxl promoters and the CpG island region. Downstream of the Gnasxl exon, CpG density falls away and the methylation pattern is complex, with partially methylated as well as unmethylated sites (Fig. 2B; 12.3-kb *Bam*HI fragment analyzed with probe X2); however, there is no marked difference between MatDp(dist2) and PatDP(dist2) DNAs. Moreover, we found no differential methylation further downstream until the DMR at *Gnas* exon 1A (29) which, as expected, showed maternal methylation in this material (data not shown). In conclusion, we have mapped the extents of the DMRs, as present in midgestation embryos, find them each to extend several kilobases and to coincide with the regions of greatest CpG density.

Extensive germ line methylation mark at the Nespas-Gnasxl DMR. A hallmark of an ICR is that distinct methylation patterns are established in male and female gametes, and differential methylation is maintained in the zygote and during embryonic development. At *Gnas*, exon 1A has been shown by bisulfite genomic sequencing to be contained in a region methylated in oocyte DNA and unmethylated in sperm DNA (29). Whether this gametic DMR controls imprinting of the entire locus, including the Nesp-Gnasxl domain, is unclear. The report from Liu et al. (29) found no evidence of gametic meth-

TABLE 1. Tandem repeats in Nesp and Gnasxl DMRs

DMR	Location[a]	Reiteration	Sequence or consensus[b]
Mouse			
Nesp	2695–2820	10 12-mers	GACTACGAGACC GAGACCGATTCT GAGACCGAGCCT GAGTCCGATATC GAGACCGAAATC GAGACCGAGCCA GAGACCGAGCCA GAAACCGAGCCA GAGACCGAGCCA GAGGACGAGCGC **GAGACCGAGCCn**
Gnasx1	16981–17196	6 36-mers	GCCGAGCCAGCCTCCGAGGCAGTCCCTGCCACCACG GCCGAGTCTGCCTCCGGGGCAGCCCCTGTCACCCAG GTGGAGCCCGCAGCCGCGGCAGTCTCTGCCACCCTG GCGGAGCCTGCCGCCCGGGCAGCCCCTATCACCCCC AAGGAGCCCACTACCCGGGCAGTCCCCTCTGCTAGA GCCCATCCGGCCGCTGGAGCAGTCCCTGGCGCCCCA **GCCGAGCCnGCCnCCCGGGCAGTCCCTGnCACCCnn** **G G**
Gnasx1	17290–17379	5 18-mers	GCTCGGGCATCCCTTCCT GCCCGCGCAGCAGCTGCC GCCCGGGCAGCCTCTGCT GCCCGCGCAGTCGCTGCT GGCCGGTCAGCCTCTGCC **GCCCGGGCAGCCnCTGCT** **C C**
Human			
NESP55	1152–1283	11 12-mers	**GAGACCGAGccC**
XLαS	14325–14564	4 60-mers	**TGaCCAgCCaGGCCTGGGAGGcTtCnGnCCAcCACTcgAACAGCCCggAgcCCTCAgTgg** **T TGG G T T TG**
XLαS	14901–15047	7 21-mers	**CGGCCCCCCnGTCGAGATnGA** **A A A**
XLαS	15154–15486	4 27-mers	**TCCGGGGCAGCCCCAGCCGATCCCGAC** **G**
XLαS	15154–15486	6 36-mers	**TCCGGGGCAGCCCCTGACGCCCCAGCCGATCCCGAC** **G**

[a] For mouse DMRs, location is based on sequence AJ251761; for human DMRs, location is based on sequence AJ251760.

[b] Boldface type indicates consensus sequence. Lowercase letters indicate predominant nucleotide, and n indicates no nucleotide >50%. Where letters are shown below consensus sequence, both nucleotides are equally likely.

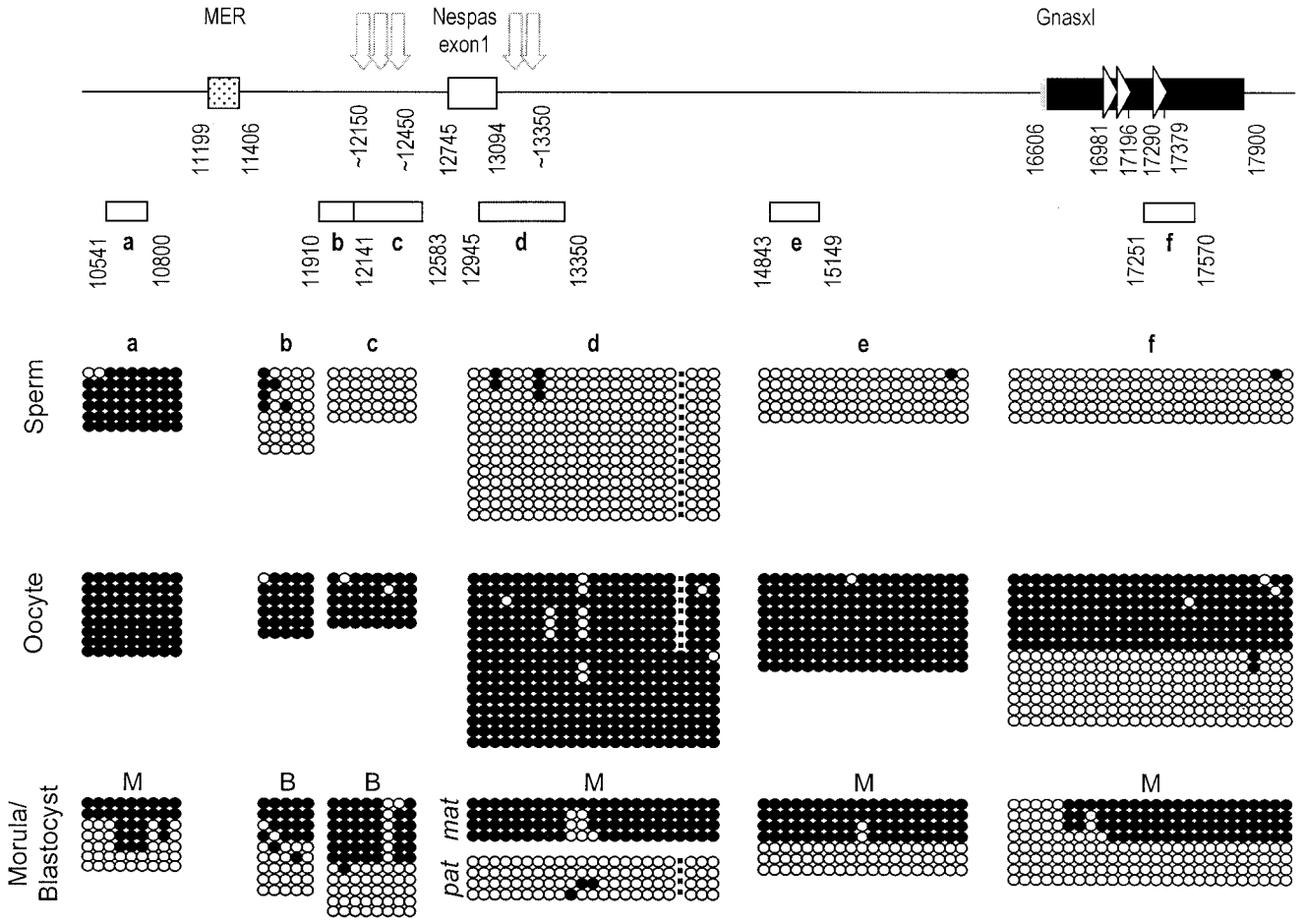

FIG. 3. Germ line and early embryo methylation of the Nespas-Gnasxl DMR. The features of the regions analyzed are indicated at the top. The Gnasxl exon is depicted as a bar with coding portion in black, untranslated in grey and direct repeats indicated by arrowheads; the Nespas exon 1 is an open box. The location of a MER DNA transposon is indicated by the stippled box. The approximate positions of HSSs present specifically on the paternal allele in ES cells are shown by vertical arrows (Fig. 6). Nucleotide positions are given according to sequence AJ251761. The extents of the PCR products sequenced after bisulfite modification of DNAs are represented by open bars labeled a to f. Methylation status is given below. Each line of circles represents an individual sequence molecule, with each circle corresponding to a separate CpG. Methylated CpGs are indicated by filled circles, nonmethylated CpGs by open circles. For PCR product d, the dot represents the position of a single-nucleotide polymorphism (5′-GGTCGG-3′ to 5′-GGTCTG-3′) found between C57BL/6J and CBA/Ca, which results in loss of the indicated CpG in the CBA/Ca sequence. Sperm DNA is from CBA/Ca and oocyte DNA from (C57BL/6J × CBA/Ca)F_1s. Morula (M) and blastocyst (B) DNAs were obtained from an $F_1 \times F_1$ cross, except for PCR product d, for which morulae were from a C57BL/6J × CBA/Ca cross, with maternal B6 allele sequences and paternal CBA allele sequences identified as *mat* and *pat*, respectively

ylation marks in the Nesp and Gnasxl DMRs, but only very limited regions were examined. We have undertaken a more extensive characterization of these regions.

Methylation in gametes and preimplantation embryos was determined by sequencing PCR products obtained from bisulfite-treated DNAs (Fig. 3). At the Nespas-Gnasxl DMR, analysis focused on two regions represented in four PCR products. PCR products b through d examined regions corresponding to prominent HSSs present specifically on the paternal allele in ES cells (see below), product d additionally examined a highly conserved region at the putative Nespas promoter (17, 27, 54), PCR product e covers the putative promoter for Gnasxl (Williamson et al., unpublished data). Bisulfite-modified sequences revealed a high level of methylation in oocyte DNA and very low levels in sperm DNA for each of these regions. In addition, sequences from preimplantation embryo DNAs (morulae or blastocysts) showed equal proportions of methylated and unmethylated sequences, suggestive of the maintenance of the oocyte and sperm derived methylation patterns after fertilization. To assign parental allele origin of the methylation present in preimplantation embryo DNAs, a C57BL/6J (B6) versus CBA/Ca (CBA) single-nucleotide polymorphism was identified in the Nespas promoter/conserved region (PCR product d). Bisulfite analysis made on DNA from morulae resulting from a B6 × CBA cross confirmed that methylated molecules were derived exclusively from the maternal allele (Fig. 3; PCR product d).

Given the extensive DMR at Nespas-Gnasxl in postimplantation embryo DNAs, we wished to ascertain whether the entire DMR was also a germ line methylation mark. Because there are few CpGs immediately upstream of PCR product b (only four CpGs in 1.1 kb), the next informative region was

further upstream between (PCR product a at positions 10541 to 10800). The highly methylated pattern found in sperm and oocyte DNA indicated that this region is no longer included in the gametic methylation mark, and the variable methylation patterns in morula DNA suggested that the region undergoes reprogramming in preimplantation stages (Fig. 3). To map the downstream border, bisulfite sequences were obtained from one block of direct repeats in the Gnasxl coding region (PCR product f). Both methylated and unmethylated sequences were obtained from oocyte DNA, and a mixture of unmethylated and mainly methylated products was recovered from morula DNA. (In the case of this PCR product, we cannot estimate the exact ratio of methylated and unmethylated sequences, as we found a bias in cloning unmethylated products, whereas restriction enzyme analysis of PCR products prior to cloning showed predominantly methylated molecules.)

For Nesp, because the promoter region had been analyzed previously (29), we obtained bisulfite sequences for two elements potentially able to attract de novo methylation: the CpG-containing direct repeats in the Nesp exon; and a B1 element (58) 2 kb downstream of Nesp. These regions were found to be unmethylated or partially methylated in sperm DNA and, where examined, were unmethylated in oocytes and morulae (data not shown). Therefore, we confirm that the Nesp DMR does not have the properties of a methylation imprint mark.

In conclusion, bisulfite sequence analysis revealed an extensive gametic methylation mark at the Nespas-Gnasxl DMR, covering >3.2 kb. The upstream extent of the methylation mark coincides with the boundary of the CpG-rich region, with the extent of the somatic DMR, and maps close to prominent ES cell-specific DNase I HSSs described below.

Investigating the chromatin organization of the Nesp-Gnasxl domain. As a further indication of elements likely to regulate imprinting of the locus, we examined chromatin organization, as revealed by hypersensitivity to DNase I in isolated nuclei. Nuclei were prepared from tissues from adult mice and from ES cell lines, as a representation of the inner cell mass of preimplantation embryos. Mice were (B6 × *M. spretus*)F_1 hybrids or backcross offspring from F_1 hybrid females to B6 males (which hereafter we refer to as *M. spretus* × B6 for simplicity), which provided restriction fragment length polymorphisms (RFLPs) to distinguish maternally derived and paternally derived alleles. The choice of tissues included those in which Nesp and Gnasxl are expressed in a significant proportion of cells, i.e., brain, and essentially nonexpressing tissues liver and kidney. Analysis of DNA methylation in these adult tissues indicated that the Nesp and Gnasxl DMRs exist essentially as in midgestation embryos (data not shown). The ES cells used were of three types and have been used previously for investigating chromatin at imprinted loci (9, 25). SF1-1 is a (B6 × CBA) × *M. spretus* hybrid cell line with paternal *M. spretus* alleles; PR-8 is derived from diploid parthenogenetic embryos which only contain oocyte-derived chromosomes; and AG-A is from androgenetic embryos which contain only sperm-derived chromosomes. The Nesp DMR was hypomethylated on both alleles in SF1-1, unmethylated in PR-8, and largely unmethylated in AG-A (Fig. 4B); the Nespas-Gnasxl DMR was unmethylated in AG-A, methylated in PR-8, and showed the appropriate differential methylation in SF1-1 (see Fig. 6). This pattern, in keeping with the finding of the bisulfite sequence analysis, is consistent with the Nespas-Gnasxl DMR being gametic in origin, while the Nesp DMR becomes established after implantation. Despite these methylation patterns, reverse transcription-PCR assays showed that Nesp was expressed specifically from the maternal allele in the hybrid ES cells SF1-1 and not detected in AG-A ES cells, and Gnasxl was expressed in AG-A ES cells and from the paternal allele in the hybrid cells (data not shown).

Imprinted chromatin features at the Nesp DMR. Chromatin organization at Nesp was analyzed in adult mouse tissues using a *Dra*I RFLP and probes D1 and D2 (Fig. 4). Hybridization with probe D1 revealed a pattern of multiple DNase I cleavages, the regularity of the pattern may suggest phasing of nucleosomes (Fig. 4). Use of probe D1 did not reveal whether the DNase I cleavages are on the maternal or paternal allele, but by comparing B6 × *M. spretus* and *M. spretus* × B6 samples the maternal allele was consistently more sensitive than the paternal allele to digestion (Fig. 4 and data not shown). Probe D2 is upstream of the *M. spretus*-specific *Dra*I site, such that the Nesp exon region is only seen on one allele with this probe. Prominent HSSs were detected with probe D2, which mapped at the putative promoter region (III) and upstream (II). These HSSs were present specifically on the maternal allele, as they appeared in the B6 × *M. spretus* samples but not in the *M. spretus* × B6 samples (Fig. 4). As all DNase I cleavages, including the promoter region HSS, were detected in the three tissues analyzed (brain and kidney are shown in Fig. 4), they appear not to be related to Nesp expression status, but rather to the imprinting of the region, possibly the fact that the maternal allele is unmethylated. In ES cells, multiple DNase I cleavages were also detected, including additional prominent HSSs mapping within Nesp exon 2 (IV) and upstream of Nesp (I and II), as well as site III at the promoter region (Fig. 4). The chromatin features were present in all three ES cell lines. As in adult tissues, therefore, DNase I sensitivity appears to coincide with hypomethylation of the locus in the ES cell lines, rather than being related to whether Nesp is expressed.

Imprinted chromatin features at the Nespas-Gnasxl DMR: prominent chromatin features specific to ES cells. The Nespas-Gnasxl region was analyzed in adult tissues using a *Sca*I RFLP in *Sca*I-*Xba*I digests (Fig. 5A). By using probe SX2 upstream of the polymorphic *Sca*I site, it was apparent that HSSs are present near the Nespas and Gnasxl promoter regions (sites IX and X) specifically on the paternal allele, and that this hypersensitivity is detected in three tissues examined (brain and liver are shown in Fig. 5A). In addition, one HSS upstream of the Nespas promoter (site VI) is present on both alleles. Hybridization with downstream probe SX1 illustrates the greater DNase I sensitivity of the paternal *versus* the maternal allele, in addition, multiple DNase I cleavages are detected across the Gnasxl exon region with this probe, which we assume to be a property of the unmethylated paternal allele.

For the hybrid ES cells SF1-1 an *Eco*RI RFLP was more informative (Fig. 6). Probe R1 revealed clusters of HSSs (VII and VIII) around Nespas exon 1 not detected in adult brain (Fig. 6A and B). As these sites were not detected using probe R2, which is downstream of the *M. spretus*-specific *Eco*RI site, they represent cleavages on the paternally derived *M. spretus* allele in SF1-1 cells. Consistent with this interpretation, similar

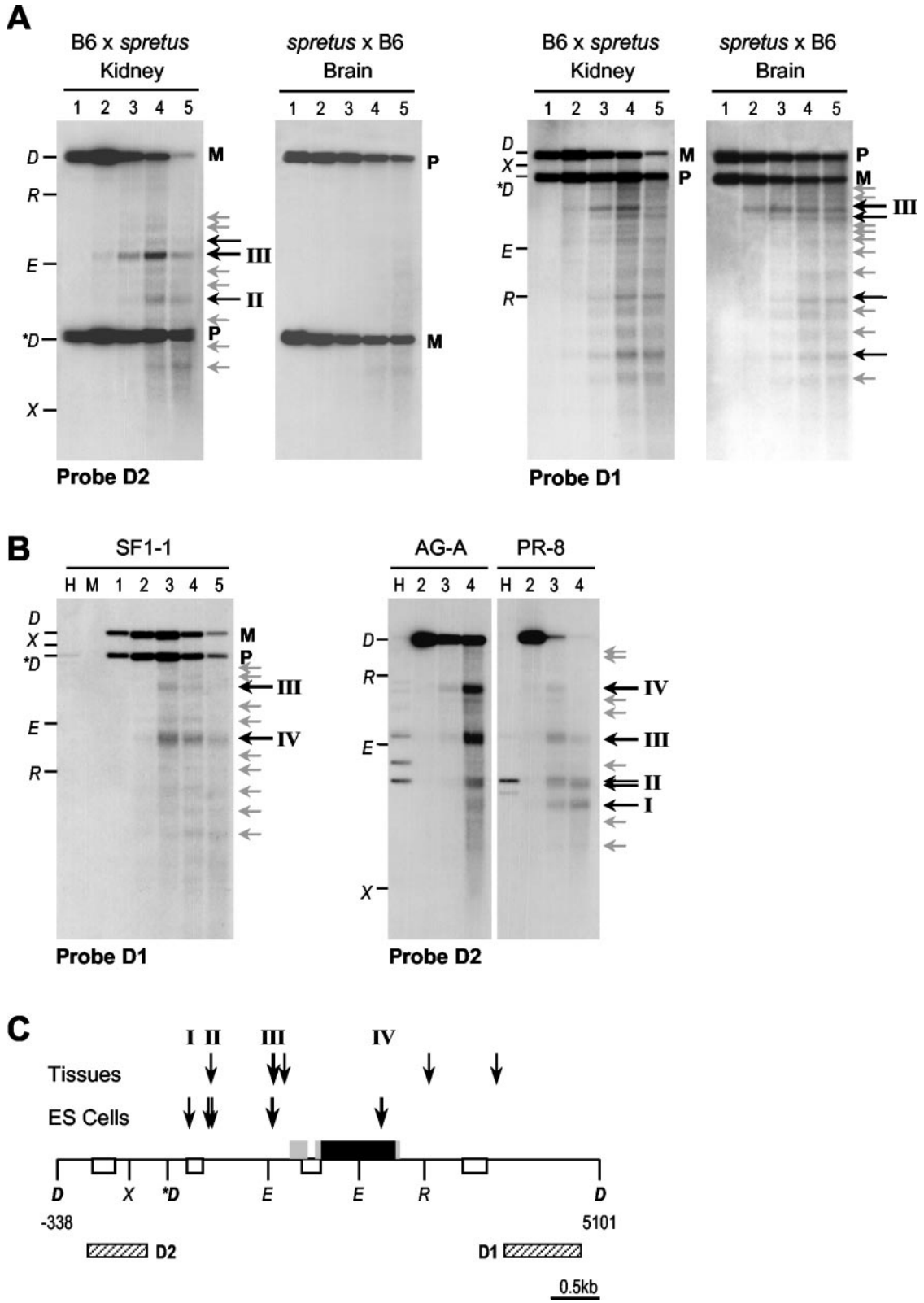

FIG. 4. DNase I hypersensitivity analysis of the Nesp region. (A) Analysis in nuclei from adult mouse kidney and brain, from (B6 × *M. spretus*) hybrids, in which the paternal allele is of *M. spretus* origin, and backcross (labeled *spretus* × B6) in which the maternal allele is *M. spretus*. Nuclei in the following lanes were digested with DNase I at the indicated concentrations: lane 1, 0 U/ml; lane 2, 50 U/ml; lane 3, 200 U/ml; lane 4, 400 U/ml; and lane 5, 750 U/ml. Purified DNA was digested with *Dra*I and electrophoresed, and Southern blots were hybridized with probes D1 or D2. Maternal (M) and paternal (P) alleles are distinguished as a *Dra*I RFLP. Points on the left of each blot represent DNA markers formed by *Dra*I (*D*)-cut DNA digested with *Eco*RI (*R*), *Eco*32I (*E*), or *Xba*I (*X*). The *M. spretus*-specific *Dra*I fragment is marked (∗*D*). Location of these

HSSs were detected in AG-A but not PR-8 cell nuclei (data not shown). Higher resolution mapping of these sites was achieved with probe M1 on *Bam*HI digests (Fig. 6C). A prominent cluster of three DNase I cleavages immediately upstream of Nespas exon 1 (VII) and two sites near the Nespas promoter (VIII) were specific to paternal alleles in ES cells. Site VII appears to coincide with the 5′ boundary of the Nespas-Gnasxl DMR. A relatively weak site (VI) was present ~1.5 kb upstream of the exon in all ES cells, as well as in adult brain, and was interpreted as a constitutive, biparental site.

DISCUSSION

Gnas is a complex imprinted locus, with five imprinted promoters associated with three DMRs. Whether imprinting of the locus is controlled by a single or multiple *cis*-acting ICRs, and where such an element(s) is located, are not yet known. In this study, we investigated potential ICRs in the Nesp-Gnasxl domain, the part of the locus where imprinting is most stringent, and where maternally expressed and paternally expressed promoters are juxtaposed. We identified a germ line DMR at which methylation is acquired in oocytes and maintained after fertilization. This gametic imprint at the Nespas-Gnasxl DMR is extensive and may cover >3.2 kb. In contrast, the DMR with paternal methylation at Nesp is established after fertilization. Both Nesp and Nespas-Gnasxl DMRs exhibit parental-allele-specific DNase I HSSs. Many of these appear to be constitutive, being present in expressing and nonexpressing tissues, and therefore reflect the parental origin or methylation status of the allele, rather than correlating directly with the activity of the promoters. In addition, particularly prominent HSSs were detected in ES cells.

***The Gnas* cluster contains two gametic methylation imprints.** As a first expectation, it might be assumed that a single ICR could suffice for the imprinting of a compact cluster such as *Gnas*. At more extended imprinted gene clusters, there are examples of more than a single germ line DMR/ICR. The distal Chr 7 imprinting cluster in mouse, and the homologous 11p15.5 region in humans associated with the Beckwith-Wiedemann syndrome, each divide into two domains with separate ICRs: at *H19*, to regulate imprinting of *Igf2* (48); and at *KvDMR1*, to regulate at least six linked imprinted transcripts (11). The former is a paternally methylated and the latter a maternally methylated gametic mark (50, 59). These elements are separated by ~750 kb, and human patient data as well as knockout work in the mouse indicate that the two elements operate as distinct ICRs to regulate nonoverlapping sets of imprinted transcripts (39). Equally, however, there are other imprinted regions that appear to be regulated by a single ICR associated with a single gametic methylation mark. At *Igf2r* an intronic DMR is required for monoallelic expression not only of the *Igf2r* promoter but also two genes 110 to 155 kb downstream (62).

Our finding that the Nespas-Gnasxl DMR is a gametic imprint, together with the earlier identification of a germ line DMR at *Gnas* exon 1A (29), therefore predicts that the locus could contain two ICRs and is divided between separate domains regulated by independent imprinting mechanisms. This possibility will need to be tested by targeting experiments in the mouse. In the meantime, support for this contention comes from imprinting anomalies of human *GNAS* encountered in the disorder PHP1b. PHP1b results from loss of GSα expression in those tissues in which expression is strictly from the maternal allele. A consistent finding in PHP1b is that the *GNAS* exon 1A DMR is unmethylated on both alleles (3, 28). Loss of imprinted methylation at exon 1A is accompanied in most patients (sporadic and familial) by normal monoallelic methylation at the NESP55 and XLαS/AS DMRs (AS is the human equivalent to Nespas), indicating that methylation at the NESP55-XLαS/AS domain can be set independently of events at exon 1A. In a few patients, however, biallelic methylation at NESP55 is seen, with or without loss of maternal methylation of XLαS/AS (3, 28), implying that in some circumstances epigenotype can be regulated in concert across the whole locus.

A second informative human condition is hydatidiform mole. Complete hydatidiform moles are normally sporadic androgenetic conceptuses, which develop without an oocyte-derived chromosome complement. In biparental complete hydatidiform mole, molar pregnancies are recurrent and the disorder is thought to arise from a defect in setting up the methylation of imprinted genes in the mother's germ line. In biparental complete hydatidiform moles analyzed to date, both the *GNAS* exon 1A DMR and AS DMR were fully unmethylated (therefore biallelically), a finding compatible with a germ line origin of either or both their normal methylation patterns, while the NESP55 DMR was fully methylated (22). It was interpreted that NESP55 is a secondary DMR, whose methylation is dependent upon absence of methylation at AS. This is consistent with our findings in mouse gametes, as well as in ES cells in which methylation was present on maternal alleles at Nespas-Gnasxl but Nesp was unmethylated.

Properties of ICRs and methylation signals. Germ line DMRs are CpG rich elements which fulfill the criteria for CpG islands, except for the unique property of acquiring methylation in the male or female germ line. What features are responsible for this methylation and for germ line selectivity? The Nespas-Gnasxl DMR seems to be typical of many gametic imprints in its association with direct repeats, although the repeat region itself was not methylated in all oocytes. Such repeats have been proposed to attract methylation de novo through possible formation of unusual DNA structures (32,

reference sites is given in C. DNase I cleavages are indicated by arrows to the right of the blots, weaker cleavages in grey, more prominent sites by the labeled black arrows. (B) Analysis in nuclei from ES cell lines (see text for description of cell lines). The key is the same as that for panel A, except that lanes marked H and M are untreated DNAs digested with *Dra*I plus *Hpa*II or *Msp*I. (C) Interpretation of DNase I HSSs. The *Dra*I fragment analyzed is shown, with nucleotide positions according to sequence AJ251761. Nesp exons are given as filled boxes, with coding portions in black and untranslated regions in grey; Nespas exons are given as open boxes. The locations of probes D1 and D2 are given as striped boxes. The approximate positions of HSSs are indicated by the vertical arrows and represent a summation of mapping with probes D1 and D2 in A and B and from additional blots (not shown).

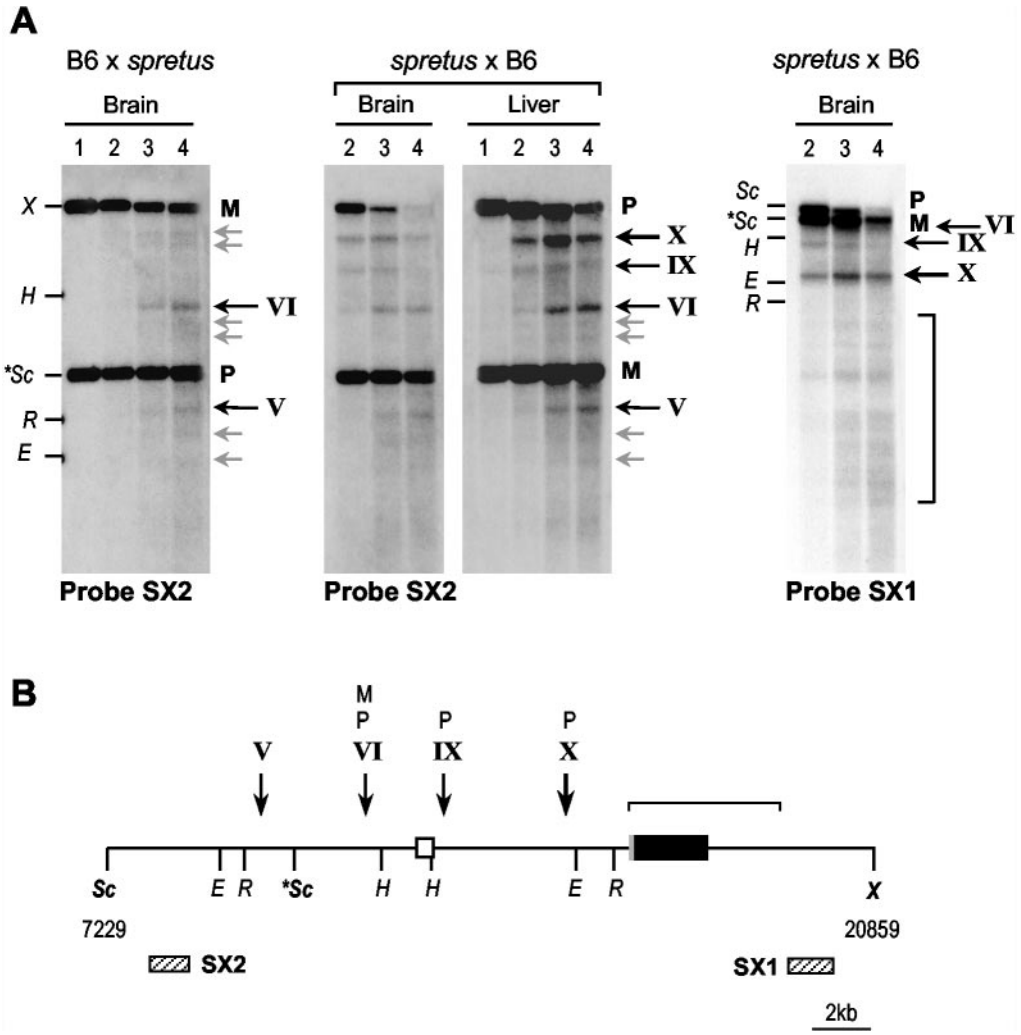

FIG. 5. DNase I hypersensitivity analysis of the Nespas-Gnasxl region in mouse tissues. (A) Analysis in nuclei from adult mouse brain and liver, from (B6 × *M. spretus*) hybrids, in which the paternal allele is *M. spretus*, and (*M. spretus* × B6) backcross, with maternal *M. spretus*. Nuclei were digested with DNase I (as in Fig. 4), purified DNA was digested with *Sca*I-*Xba*I and electrophoresed, and Southern blots were hybridized with probe SX2 or SX1. Maternal (M) and paternal (P) alleles are distinguished as a *Sca*I RFLP. Points on the left of the blots represent DNA markers formed by *Sca*I (*Sc*)-cut DNA digested with *Xba*I (*X*), *Eco*RI (*R*), *Hin*dIII (*H*), or *Eco*32I (*E*). The *M. spretus*-specific *Sca*I fragment is given (∗*Sc*). Location of these reference sites is shown in panel B. DNase I cleavages are indicated by arrows to the right of each blot, weaker cleavages in grey, more prominent sites in black. (B) Interpretation of DNase I HSSs. The *Sca*I-*Xba*I fragment analyzed is shown. The Gnasxl exon is given as the black box, with 5′ untranslated region in grey; the Nespas exon 1 is shown as the open box. The locations of probes SX1 and SX2 are given as striped boxes. The DNase I HSSs mapped from these and additional blots (not shown) are indicated using the convention above. HSSs on the maternal or paternal allele are labeled M or P, respectively.

40). Members of the Dnmt3 family are required for methylation at DMRs in oocytes (6, 15), but whether they respond to such repeats has not been shown. The most persuasive evidence for the involvement of direct repeats comes from *Rasgrf1*, whose paternal-specific expression is controlled by a remote DMR whose sperm-derived methylation depends upon a direct repeat block (60). In contrast, a GC-rich repeat in *H19* appears to be dispensable for imprinting (38, 49). These pertain to paternal methylation, and for maternally methylated DMRs decisive tests through targeting have not been reported, although the direct repeat region of the *U2af1-rs1* DMR appears to be superfluous (46). In the context of a synthetic transgene construct, the *Igf2r/Air* DMR can act as an imprinted methylation signal, this activity residing in the direct repeat region (40). However, the *Igf2r/Air* DMR imprints very inefficiently as a transgene in its own right (42), suggesting that elements in addition to the direct repeats are necessary for attracting or maintaining methylation allele-specifically. Direct repeats may facilitate the spread of methylation from surrounding regions undergoing methylation de novo in the germ lines. At the Nespas-Gnasxl DMR, as well as those at *U2af1-rs1*, *Rasgrf1* and *Grb10* (1, 41), methylation was present immediately upstream of the DMR in both germ lines. It will be important to track the time of appearance of methylation during germ cell development to see whether methylation of the DMR occurs in concert with that of the surrounding sequences, which would favor a spreading model. Alternatively, the spread of methylation may be limited in one germ line by

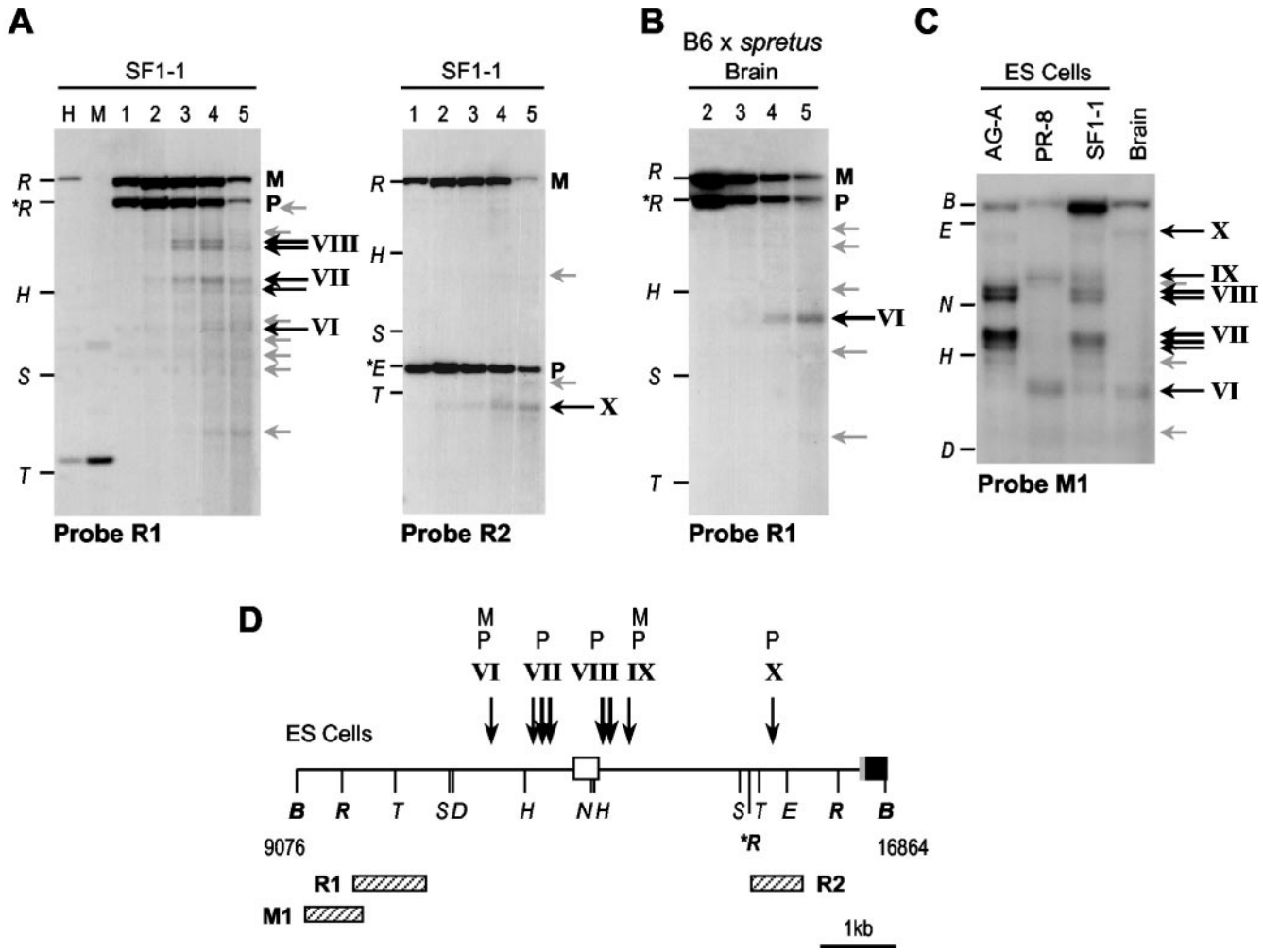

FIG. 6. DNase I analysis of the Nespas promoter region in ES cells. (A) Analysis of nuclei from SF1-1 ($F_1 \times$ *M. spretus*) ES cells, using an *Eco*RI RFLP. Nuclei were digested with DNase I (as in Fig. 4), purified DNA was digested with *Eco*RI and electrophoresed, and Southern blots were hybridized with probes R1 and R2. Maternal (M) and paternal (P) alleles are indicated to the right of the blot. Points on the left of the blot represent DNA markers formed by *Eco*RI (*R*) cut DNA separately digested with *Hin*dIII (*H*), *Sac*I (*S*) or *Taq*I (*T*). The *M. spretus*-specific *Eco*RI fragment is given as ∗*R*. Location of these reference sites is shown in D. DNase I cleavages are indicated by arrows to the right of each blot, weaker cleavages in grey, more prominent sites in black. Lanes marked H and M are untreated DNAs digested with *Eco*RI plus *Hpa*II or *Msp*I. (B) Similar analysis in nuclei from adult mouse brain (B6 × *M. spretus* hybrid). (C) Analysis using probe M1 in *Bam*HI digested DNAs, for fine mapping of the ES cell-specific HSSs. Restriction site markers are *Bam*HI (B), *Hin*dIII (*H*), *Nco*I (*N*), *Eco*32I (*E*) and *Taq*I (*T*). (D) Interpretation of DNase I HSSs. The start of the Gnasxl exon is represented as a filled box with 5′ untranslated region in grey, Nespas exon 1 as the open box. Locations of probes M1, R1 and R2 are given as striped boxes. The DNase I sites mapped from these and additional blots (not shown) are indicated using the convention above. HSSs on the maternal allele are labeled M, on the paternal allele P.

factors bound to the DNA. The 5′ border of the Nesp-Gnasxl DMR is associated with prominent HSSs on the sperm-derived allele in ES cells, but whether such HSSs are also present specifically during male gametogenesis and could provide an impediment to methylation remains to be shown.

At most ICRs studied to date, parental-allele-specific methylation is accompanied by parental-allele-specific chromatin features. These include DNase I HSSs likely to reflect the binding of methylation-sensitive nonhistone proteins on the unmethylated allele, methyl-cytosine binding proteins on the unmethylated allele, as well as differences in histone modifications (10, 12). Only in the case of the Angelman syndrome region is there evidence for an ICR demarcated by differential chromatin organization in the absence of differential methylation (35). Both DMRs in the Nesp-Gnasxl domain were associated with HSSs in adult tissues, most of which were present constitutively on the unmethylated allele. We looked specifically for HSSs in ES cells, because these cells represent an early embryonic state, a stage at which the maintenance of differential methylation against the genome-wide changes in methylation is critical, and because the availability of androgenetic and parthenogenetic ES cells allowed us to examine maternal and paternal alleles separately. Furthermore, studies at *H19* revealed that pivotal elements in the imprinting of the locus are recognized as prominent HSSs in these cells (25, 47). Strong HSS were indeed identified at the Nespas-Gnasxl DMR, which flanked the putative start site for Nespas, and were present specifically on paternally derived, unmethylated

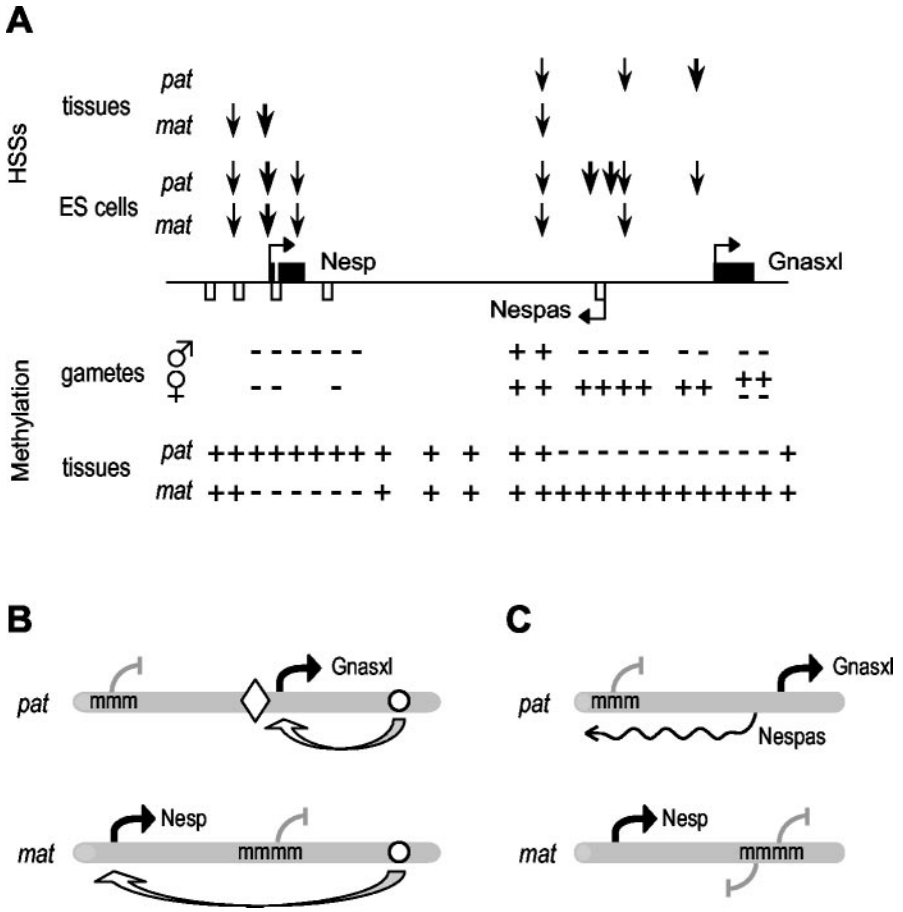

FIG. 7. Epigenetic features and models of reciprocal imprinted expression of Nesp and Gnasxl. (A) Summary of epigenetic features. The Nesp, Nespas and Gnasxl exons are depicted as before. Above the line, the approximate locations of DNase I HSSs are marked by the vertical arrows, with thickness of arrow reflecting prominence of HSS, and are shown for maternal (*mat*) and paternal (*pat*) alleles in adult tissues and ES cells. Below the line, methylation status is summarized, in both gametes and embryonic tissues, with methylated regions (+) and unmethylated regions (−) marked. (B) Enhancer-boundary model for monoallelic expression of Nesp and Gnasxl. Methylated promoters are indicated (mmm). The open circle represents the position of hypothetical enhancers able to control the Nesp and Gnasxl promoters, and the diamond a methylation-sensitive boundary. Active promoters are indicated by the black arrows. (C) Antisense model. Expression of the Nespas antisense is indicated by the wavy line. See text for description of the models.

alleles. It will be an important future aim to determine the identity of the protein-DNA interactions at these sites.

Models for imprinted expression of Nesp and Gnasxl. Collecting our observations together, we consider two models for the reciprocal imprinting of the Nesp and Gnasxl promoters (Fig. 7). In the first model, the Nespas-Gnasxl DMR is a gametic mark and represents a boundary, in the manner of the *H19* insulator (4, 14). The essential elements of the model are: the Nesp and Gnasxl promoters have similar expression profiles (predominantly neuroendocrine tissues) (21, 23); the germ line DMR covers the Gnasxl promoter and the boundary element; the boundary is predicted to operate in a methylation-sensitive fashion. On the paternal allele, binding of insulator factors occurs which limit the action of downstream enhancers (yet to be characterized) to the unmethylated Gnasxl promoter. The Nesp promoter is thus quiescent and methylation ensues secondary to promoter inactivity. On the maternal allele, the Gnasxl promoter is silenced by methylation, the boundary fails to establish and downstream enhancers are free to interact with the unmethylated Nesp promoter. Relevant to this model, particularly prominent HSSs at the Nespas/Gnasxl DMR were found in ES cells but not adult tissues. This might suggest that the predicted boundary is functional in early embryonic cells, but becomes redundant once methylation at Nesp and Gnasxl is firmly set up so that differential enhancer access is controlled directly by the robust methylation and accompanying chromatin changes at the promoters. The methylation-sensitive boundary elements of the *H19* and *Peg3* imprinted genes comprise reiterated binding sites for the multifunctional DNA binding factors CTCF and YY1, respectively (4, 14, 26). In the Nesp-Gnasxl domain, we did not find similar clustered binding sites mapping within repeat arrays or within the HSSs. Isolated imperfect matches to CTCF and YY1 binding motifs were found throughout the mouse Nesp-Gnasxl domain, but these were not conserved in the human sequence, except for a pair of putative CTCF binding sites at the Nesp and NESP55 promoter regions (data not shown). Therefore, the nature of the factors at a hypothetical boundary would need to be investigated further. A second model draws analogies from the *Igf2r* locus and regulation by the antisense tran-

script *Air* (56). In this scenario, the Nespas-Gnasxl DMR is a unidirectional, *cis*-acting silencer on the unmethylated paternal allele, being the start site for the paternally expressed Nespas transcript antisense to Nesp. Expression of Nespas prevents expression of the Nesp promoter in *cis*, possibly by organization of a repressive chromatin structure or by inducing methylation. One difficulty with the antisense model is the imperfect concordance between sites of Nespas and Nesp expression (2, 27). These studies examined midgestation embryos or adult tissues, however, and do not exclude a model in which Nespas expression is required specifically at early stages to establish monoallelic expression and initiate permanent silencing of the Nesp promoter (via methylation and chromatin changes), after which Nespas may be redundant. Functional tests using gene targeting and other assays will need to be done to differentiate among these and alternative models.

ACKNOWLEDGMENTS

C.C. and P.A. contributed equally to this work.

We are sincerely grateful to J. Richard Chaillet (Rangos Research Center, Pittsburgh) for advice in setting up bisulfite sequencing analysis from mouse germ cells. We thank Simon Ball (Harwell) for *M. spretus* stocks and Nick Allen (Babraham) for uniparental ES cell lines. We also thank Rachel Smith for helpful comments on the manuscript.

P.A. is supported by a Marie Curie Individual Fellowship from the European Community Programme in Human Potential (under contract HPMF-CT-2001-01122); C.C. and E.A.C. were supported by studentships from the MRC and BBSRC. G.K. is a senior fellow of the MRC.

REFERENCES

1. **Arnaud, P., D. Monk, M. Hitchins, E. Gordon, W. Dean, C. V. Beechey, J. Peters, W. Craigen, M. Preece, P. Stanier, G. E. Moore, G. E., and G. Kelsey.** 2003. Conserved methylation imprints in the human and mouse *GRB10* genes with divergent allelic expression suggests differential reading of the same mark. Hum. Mol. Genet. **12:**1005–1019.
2. **Ball, S. T., C. M. Williamson, C. Hayes, T. Hacker, and J. Peters.** 2001. The spatial and temporal expression pattern of *Nesp* and its antisense *Nespas*, in mid-gestation mouse embryos. Mech. Dev. **100:**79–81.
3. **Bastepe, M., J. E. Pincus, T. Sugimoto, K. Tojo, M. Kanatani, Y. Azuma, K. Kruse, A. L. Rosenbloom, H. Koshiyama, and H. Jüppner.** 2001. Positional dissociation between the genetic mutation responsible for pseudohypoparathyroidism type 1b and the associated methylation defect at exon A/B: evidence for a long-range regulatory element within the imprinted *GNAS1* locus. Hum. Mol. Genet. **10:**1231–1241.
4. **Bell, A. C., and G. Felsenfeld.** 2000. Methylation of a CTCF-dependent boundary controls imprinted expression of the *Igf2* gene. Nature **405:**482–485.
5. **Benson, G.** 1999. Tandem Repeats Finder: a program to analyze DNA sequences. Nucleic Acids Res. **15:**573–580.
6. **Bourc'his, D., G.-L. Xu, C.-S. Lin, B. Bollman, and T. H. Bestor.** 2001. Dnmt3L and the establishment of maternal genomic imprints. Science **294:**2536–2539.
7. **Cattanach, B. M., and M. Kirk.** 1985. Differential activity of maternally and paternally derived chromosome regions in mice. Nature **315:**496–498.
8. **Davies, S. J., and H. E. Hughes.** 1993. Imprinting of Albright's hereditary osteodystrophy. J. Med. Genet. **30:**101–103.
9. **Feil, R., M. D. Boyano, N. D. Allen, and G. Kelsey.** 1997. Parental chromosome-specific chromatin conformation in the imprinted *U2af1-rs1* gene in the mouse. J. Biol. Chem. **272:**20893–20900.
10. **Feil, R., and S. Khosla.** 1999. Genomic imprinting in mammals: an interplay between chromatin and DNA methylation? Trends Genet. **15:**431–435.
11. **Fitzpatrick, G. V., P. D. Soloway, and M. J. Hughes.** 2002. Regional loss of imprinting and growth deficiency in mice with a targeted deletion of. KvDMR1. Nat. Genet. **32:**426–431.
12. **Fournier, C., Y. Goto, E. Ballestar, K. Delaval, A. M. Hever, M. Esteller, and R. Feil.** 2002. Allele-specific histone lysine methylation marks regulatory regions at imprinted mouse genes. EMBO J. **21:**6560–6570.
13. **Germain-Lee, E. L., C. L. Ding, Z. Deng, J. L. Crane, M. Saji, M. D. Ringel, and M. A. Levine.** 2002. Paternal imprinting of Galpha(s) in the human thyroid as the basis of TSH resistance in pseudohypoparathyroidism type 1a. Biochem. Biophys. Res. Commun. **296:**67–72.
14. **Hark, A. T., C. J. Schoenherr, D. J. Katz, R. S. Ingram, J. M. Levorse, and S. M. Tilghman.** 2000. CTCF mediates methylation-sensitive enhancer-blocking activity at the *H19/Igf2* locus. Nature **405:**486–489.
15. **Hata, K., M. Okano, H. Lee, and E. Li.** 2002. Dnmt3L cooperates with the Dnmt3 family of de novo DNA methyltransferases to establish maternal imprints in mice. Development **129:**1983–1993.
16. **Hayward, B. E., A. Barlier, M. Korbonits, A. B. Grossman, P. Jacquet, A. Enjalbert, and D. T. Bonthron.** 2001. Imprinting of the $G_s\alpha$ gene *GNAS1* in the pathogenesis of acromegaly. J. Clin. Investig. **107:**R31–R36.
17. **Hayward, B. E., and D. T. Bonthron.** 2000. An imprinted antisense transcript at the human *GNAS1* locus. Hum. Mol. Genet. **9:**835–841.
18. **Hayward, B. E., M. Kamiya, L. Strain, V. Moran, R. Campbell, Y. Hayashizaki, and D. T. Bonthron.** 1998. The human *GNAS1* gene is imprinted and encodes distinct paternally and biallelically expressed G proteins. Proc. Natl. Acad. Sci. **95:**10038–10043.
19. **Hayward, B. E., V. Moran, L. Strain, and D. T. Bonthron.** 1998. Bidirectional imprinting of a single gene: *GNAS1* encodes maternally, paternally, and biallelically derived proteins. Proc. Natl. Acad. Sci. **95:**15475–15480.
20. **Hogan, B., R. Beddington, F. Costantini, and E. Lacy.** 1994. Manipulating the mouse embryo: a laboratory manual. Cold Spring Harbor Laboratory Press, Cold Spring Harbor, N.Y.
21. **Ischia, R., P. Lovisetti-Scamihorn, R. Hogue-Angeletti, M. Wolkersdorfer, H. Winkler, and R. Fisher-Colbrie.** 1997. Molecular cloning and characterisation of NESP55, a novel chromogranin-like precursor of a peptide with 5-HT_{1B} receptor antagonist activity. J. Biol. Chem. **272:**11657–11662.
22. **Judson, H., B. E. Hayward, E. Sheridan, and D. T. Bonthron.** 2002. A global disorder of imprinting in the human female germ line. Nature **416:**539–542.
23. **Kehlenbach, R. H., J. Matthey, and W. B. Huttner.** 1994. XLαs is a new type of G protein. Nature **372:**804–809.
24. **Kelsey, G., D. Bodle, H. J. Miller, C. V. Beechey, C. Coombes, J. Peters, and C. M. Williamson.** 1999. Identification of imprinted loci by methylation-sensitive representational difference analysis: application to mouse distal chromosome 2. Genomics **62:**129–138.
25. **Khosla, S., A. Aitchison, R. Gregory, N. D. Allen, and R. Feil.** 1999. Parental allele-specific chromatin configuration in a boundary-imprinting-control element upstream of the mouse *H19* gene. Mol. Cell. Biol. **19:**2556–2566.
26. **Kim, J., A. Kollhoff, A. Bergmann, and L. Stubbs.** 2003. Methylation-sensitive binding of transcription factor YY1 to an insulator sequence within the paternally expressed imprinted gene *Peg3.* Hum. Mol. Genet. **12:**233–245.
27. **Li, T., T. H. Vu, Z.-L. Zeng, B. T. Nguyen, B. E. Hayward, D. T. Bonthron, J.-F. Hu, and A. R Hoffman.** 2000. Tissue-specific expression of antisense and sense transcripts at the imprinted *Gnas* locus. Genomics **69:**295–304.
28. **Liu, J., D. Litman, M. J. Rosenberg, S. Yu, L. G. Biesecker, and L. S. Weinstein.** 2000. A *GNAS1* imprinting defect in pseudohypoparathyroidism type 1B. J. Clin. Investig. **106:**1167–1174.
29. **Liu, J., S. Yu, D. Litman, W. Chen, and L. S. Weinstein.** 2000. Identification of a methylation imprint mark within the mouse *Gnas* locus. Mol. Cell. Biol. **20:**5808–5817.
30. **Mantovani, G., E. Ballare, E. Giammona, P. Beck-Peccoz, and A. Spada.** 2002. The Gsα gene: predominant maternal origin of transcription in human thyroid gland and gonads. J. Clin. Endocrin. Metab. **87:**4736–4740.
31. **Morison, I. M., C. J. Paton, and S. D. Cleverley.** 2001. The imprinted gene and parent-of-origin effect database. Nucleic Acids Res. **29:**275–276.
32. **Neumann, B., P. Kubicka, and D. P. Barlow.** 1995. Characteristics of imprinted genes. Nat. Genet. **9:**12–13.
33. **Okamura, K., Y. Hagiwara-Takeuchi, T. Li, T. H. Vu, M. Hirai, M. Hattori, Y. Sakaki, A. R. Hoffman, and T. Ito.** 2000. Comparative genome analysis of the mouse imprinted gene impact and its nonimprinted human homolog IMPACT: toward the structural basis for species-specific imprinting. Genome Res. **10:**1878–1889.
34. **Pearsall, R. S., C. Plass, M. A. Romano, M. D. Garrick, H. Shibata, Y. Hayashizaki, and W. A. Held.** 1999. A direct repeat sequence at the *Rasgrf1* locus and imprinted expression. Genomics **55:**194–201.
35. **Perk, J., K. Makedonski, L. Lande, H. Cedar, A. Razin, and R. Shemer.** 2002. The imprinting mechanism of the Prader-Willi/Angelman regional control center. EMBO J. **21:**5807–5814.
36. **Peters, J., C. V. Beechey, S. T. Ball, and E. P. Evans.** 1994. Mapping studies of the distal imprinting region of mouse chromosome 2. Genet. Res. **63:**169–174.
37. **Peters, J., S. F. Wroe, C. A. Wells, H. J. Miller, D. Bodle, C. V. Beechey, C. M. Williamson, C. M. Williamson, and G. Kelsey.** 1999. A cluster of novel oppositely imprinted transcripts at the *Gnas* locus in the distal imprinting region of mouse chromosome 2. Proc. Natl. Acad. Sci. **96:**3830–3835.
38. **Reed, M. R., A. D. Riggs, and J. R. Mann.** 2001. Deletion of a direct repeat element has no effect on *Igf2* and *H19* imprinting. Mamm. Genome **12:**873–876.
39. **Reik, W., and J. Walter.** 2001. Genomic imprinting: parental influence on the genome. Nat. Rev. Genet. **2:**21–32.
40. **Reinhart, B., M. Eljanne, and J. R. Chaillet.** 2002. Shared role for differentially methylated domains of imprinted genes. Mol. Cell. Biol. **22:**2089–2098.
41. **Shibata, H., Y. Yoda, R. Kato, T. Ueda, M. Kamiya, N. Hiraiwa, A. Yoshiki, C. Plass, R. S. Pearsall, W. A. Held, M. Muramatsu, H. Sasaki, M. Kusakabe, and Y. Hayashizaki.** 1998. A methylation imprint mark in the mouse

imprinted gene *Grf1*/*Cdc25Mm* locus shares a common feature with the *U2afbp-rs* gene: an association with a short tandem repeat and a hypermethylated region. Genomics **49:**30–37.
42. **Sleutels, F., and D. P. Barlow.** 2001. Investigation of elements sufficient to imprint the mouse *Air* promoter. Mol. Cell. Biol. **21:**5008–5017.
43. **Sleutels, F., and D. P. Barlow.** 2002. The origins of genomic imprinting in mammals. Adv. Genet. **46:**119–163.
44. **Smith, R. J., P. Arnaud, G. Konfortova, W. L. Dean, C. V. Beechey, C. V. Beechey, and G. Kelsey.** 2002. The mouse *Zac1* locus: basis for imprinting and comparison with human *ZAC.* Gene **292:**101–112.
45. **Stöger, R., P. Kubicka, C.-G. Liu, T. Kafri, A. Razin, H. Cedar, and D. P. Barlow.** 1993. Maternal-specific methylation of the imprinted mouse *Igf2r* locus identifies the expressed locus as carrying the imprinting signal. Cell **73:**61–71.
46. **Sunahara, S., K. Nakamura, K. Nakao, Y. Gondo, Y. Kagata, and M. Katsuki.** 2000. The oocyte-specific methylated region of the *U2afbp-rs*/*U2af1-rs1* gene is dispensible for its imprinted methylation. Biochem. Biophys. Res. Commun. **268:**590–595.
47. **Szabó, P. E., G. P. Pfeifer, and J. R. Mann.** 1998. Characterization of novel parent-specific epigenetic modifications upstream of the imprinted mouse *H19* gene. Mol. Cell. Biol. **18:**6767–6776.
48. **Thorvaldsen, J. L., K. L. Duran, and M. S. Bartolomei.** 1998. Deletion of the H19 differentially methylated domain results in loss of imprinted expression of *H19 and. Igf2.* Genes Dev. **12:**3693–3702.
49. **Thorvaldsen, J. L., M. R. W. Mann, O. Nwoko, K. L. Duran, and M. S. Bartolomei.** 2002. Analysis of sequence upstream of the endogenous *H19* gene reveals elements both essential and dispensable for imprinting. Mol. Cell. Biol. **22:**2450–2462.
50. **Tremblay, K. D., J. R. Saam, R. S. Ingram, S. M. Tilghman, and M. S. Bartolomei.** 1995. A paternal-specific methylation imprint marks the alleles of the mouse *H19* gene. Nat. Genet. **9:**407–413.
51. **Tycko, B., and I. M. Morison.** 2002. Physiological functions of imprinted genes. J. Cell. Physiol. **192:**245–258.
52. **Weinstein, L. S., S. Yu, D. R. Warner, and J. Liu.** 2001. Endocrine manifestations of stimulatory G protein alpha-subunit mutations and the role of genomic imprinting. Endocr. Rev. **22:**675–705.
53. **Williamson, C. M., C. V. Beechey, S. T. Ball, E. R. Dutton, B. M. Cattanach, C. Tease, F. Ishino, and J. Peters.** 1998. Localisation of the imprinted gene neuronatin, Nnat, confirms and refines the location of a second imprinting region on mouse chromosome 2. Cytogenet. Cell. Genet. **81:**73–78.
54. **Williamson, C. M., J. A. Skinner, G. Kelsey, G. Kelsey, and J. Peters.** 2002. Alternative non-coding splice variants of to *Nespas*, an imprinted gene antisense to *Nesp* in the *Gnas* imprinting cluster. Mamm. Genome **13:**74–79.
55. **Wroe, S. F., G. Kelsey, J. A. Skinner, D. Bodle, S. T. Ball, C. V. Beechey, J. Peters, and C. M. Williamson.** 2000. An imprinted transcript, antisense to *Nesp*, adds complexity to the cluster of imprinted genes at the mouse *Gnas* locus. Proc. Natl. Acad. Sci.USA **97:**3342–3346.
56. **Wutz, A., O. W. Smrzka, N. Schweifer, K. Schellander, E. F. Wagner, and D. P. Barlow.** 1997. Imprinted expression of the Igf2r gene depends on an intronic CpG island. Nature **389:**745–749.
57. **Wylie, A. A., S. K. Murphy, T. C. Orton, and R. L. Jirtle.** 2000. Novel imprinted *DLK1*/*GTL2* domain on human chromosome 14 contains motifs that mimic those implicated in *Igf2*/*H19* regulation. Genome Res. **10:**1711–1718.
58. **Yates, P. A., R. W. Burman, P. Mummanemi, S. Krussel, and M. S. Turker.** 1999. Tandem B1 elements located in a mouse methylation center provide a target for *de novo* DNA methylation. J. Biol. Chem. **274:**36357–36361.
59. **Yatsuki, H., K. Joh, K. Higashimoto, H. Soejima, Y. Arai, Y. Wang, H. Hatada, Y. Obata, H. Morisaki, Z. Zhang, T. Nakgawachi, Y. Satoh, and T. Mukai.** 2002. Domain regulation of imprinting cluster in *Kip2*/*Lit1* subdomain on mouse chromosome 7F4/F5: large-scale DNA methylation analysis reveals that DMR-Lit1 is a putative imprinting control region. Genome Res. **12:**1860–1870.
60. **Yoon, B., J., H. Herman, A. Sikora, L. T. Smith, C. Plass, and P. D. Soloway.** 2002. Regulation of DNA methylation of Rasgrf1. Nat. Genet. **30:**92–96.
61. **Yu, S., D. Yu, E. Lee, M. Eckhaus, R. Lee, Z. Corria, D. Accili, H. Westphal, and L. S. Weinstein.** 1998. Variable and tissue-specific hormone resistance in heterotrimeric Gs protein α-subunit ($G_s\alpha$) knockout mice is due to tissue-specific imprinting of the $G_s\alpha$ gene. Proc. Natl. Acad. Sci. USA **95:**8715–8720.
62. **Zwart, R., F. Sleutels, A. Wutz, A. H. Schinkel, and D. P. Barlow.** 2001. Bidirectional action of the *Igf2r* imprint control element on upstream and downstream imprinted genes. Genes Dev. **15:**2361–2366.